Persistent photoconductivity in strained epitaxial $BiFeO_3$ thin films

Akash Bhatnagar,[*,†] Young Heon Kim,[‡] Dietrich Hesse,[†] and Marin Alexe[†,¶]

Max Planck Institute of Microstructure Physics, Weinberg 2, 06120 Halle, Germany, Korea Research Institute of Standards and Science, Daejeon 305-340, Republic of Korea, and University of Warwick, Coventry CV4 7AL, United Kingdom

E-mail: bhatnaga@mpi-halle.mpg.de

Abstract

A drastic change in the conductivity of strained $BiFeO_3$ (BFO) films is observed after illuminating them with above-band gap light. This has been termed as persistent photoconductivity. The enhanced conductivity decays exponentially with time. A trapping character of the sub-band levels and their subsequent gradual emptying is proposed as a possible mechanism.

Keywords

$BiFeO_3$, strain, enhanced conductivity, persistent photoconductivity, thermally stimulated current

Strained $BiFeO_3$ (BFO) has proven to show intriguing properties, many of which are very different from the parent non-strained BFO phase. BFO is generally known to have a

[*]To whom correspondence should be addressed
[†]Max Planck Institute of Microstructure Physics, Weinberg 2, 06120 Halle, Germany
[‡]Korea Research Institute of Standards and Science, Daejeon 305-340, Republic of Korea
[¶]University of Warwick, Coventry CV4 7AL, United Kingdom

rhombohedrally distorted perovskite structure with the space group R3c.[1] Epitaxial growth of BFO (pseudo cubic lattice parameter a_{pc}= 3.96 Å) on $LaAlO_3$ (LAO) (a_{pc}=3.78 Å) is realized under a large compressive stress due to a 4.4% lattice mismatch. Owing to the mismatch, BFO crystallizes in a tetragonal-like phase with a monoclinic distortion and an enhanced c/a ratio of 1.23.[2,3] First-principle calculations predict this phase to exhibit large polarization values of 150 μC/cm^2 which are much larger compared to the values obtained for fully strained PZT.[4] Subsequent studies revealed that the tetragonal-like phase is actually a monoclinic phase which can be subcategorized as the M_c phase.[5,6] With an increase in film thickness, another variant of monoclinic structure begins to evolve in the form of lamellas/stripes which are embedded in the matrix of the original M_c phase.[5] The possibility to electrically switch between these two phases, thereby producing efficient electromechanical responses, makes the strained system of BFO a rather attractive lead-free alternative for several applications.[7] Additionally, BFO is a wide band gap (≈ 2.7 eV) oxide semiconductor which allows electronic applications, like resistive switching.[8] Recently, Mössbauer studies revealed a simplified magnetic structure in the strained BFO films and hence they can be of great interest for future spintronic and magnonic devices.[9–11] Keeping in perspective the significant changes in general physical properties such as symmetry, ferroelectricity and magnetic structure induced by strain, one may also presume a significant variation in the electronic structure.

Here we show an important effect of strain on the electronic properties of BFO films. In particular, we show an enhancement of almost three orders of magnitude in the conductivity of strained BFO films after illuminating them with light of photon energy slightly higher than the band gap. This enhanced conductivity persisted over a period of time which exceeded many hours. Lately, such enhanced and persistent photoconductivity (PPC) has also been reported at the interface between two wide-band gap insulators, i.e. $SrTiO_3$ (STO) and $LaAlO_3$ (LAO)[12,13] (which are also known to exhibit a quasi-two-dimensional electron gas),[14,15] and in STO crystals annealed at high temperature.[16] In these cases the PPC has

been observed either due to an interfacial property or due to a deliberate formation of defect levels.[16] Here we show the manifestation of the persistent photoconductivity in BFO films as a strain-induced effect.

Film and structure

BFO films with nominal thickness of 110 nm and $(001)_{pc}$-orientation were deposited by pulsed laser deposition on bare LAO $(001)_{pc}$ substrates. Details about the film growth can be found in the Methods section. Figure 1a shows an atomic force microscopy (AFM) image of a 110 nm thick BFO film grown on LAO. The morphology shows a rather complex pattern with lamella-like structures embedded in the film matrix. For detailed structural analysis, we performed reciprocal space map (RSM) studies around the $(103)_{pc}$ plane which is shown in Figure 1c. The RSM clearly depicts the epitaxial growth of BFO on LAO with an out-of-plane lattice parameter of BFO in the range of 4.6 to 4.7 Å. The corresponding c/a ratio is approximately 1.23. Moreover, the three-fold splitting of the BFO peak that is visible in the RSM is a clear hint to the M_c phase.[5,6] The cross-sectional TEM micrograph shown in Figure 1b indicates the epitaxial nature of the film and the abrupt film/substrate interface.

Persistent photoconductivity

Pristine BFO films show rather low conductivity. Figure 2a shows IV (current-voltage) characteristics for a 110 nm thick BFO film deposited on LAO. Before subjection to any kind of illumination the IV curve is linear, with the current ranging within 1-2 pA when the voltage is varied up to 15 V. The corresponding conductivity is 0.85 nS/cm. However, the conductivity is markedly enhanced after illuminating the measurement gap for 20 minutes with light of photon energy above the band gap of BFO ($h\upsilon$=3.06 eV) and subsequently switching off the illumination. As can be observed from Figure 2a, the IV curve which was measured immediately after switching off the illumination has a conductivity value of

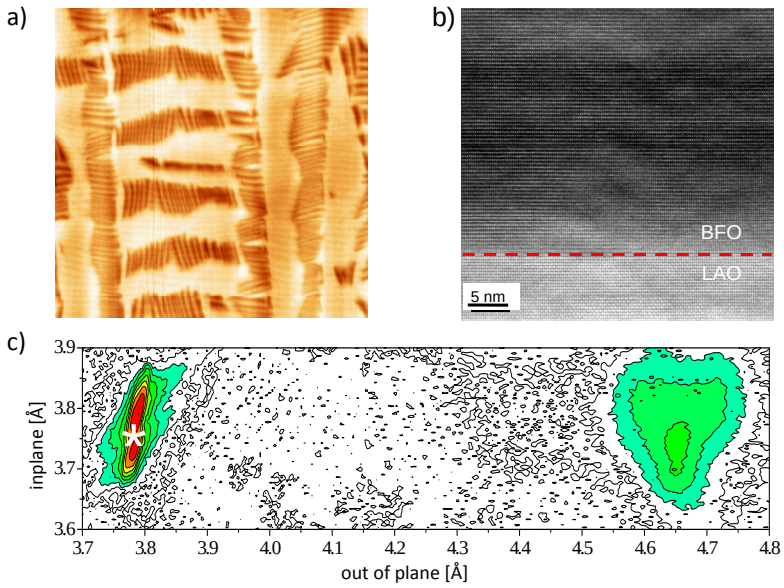

Figure 1: a) AFM image of size 3.8x3.8 μm for an approx. 110 nm thick BFO film grown on LAO substrate. b) Cross-sectional TEM micrograph of a region free from the lamellae shown in (a), showing the interface between the BFO film and the LAO substrate. c) RSM measured around $(103)_{pc}$ for an approximately 100 nm thick BFO film grown on LAO. The peak from the substrate is marked with a white star.

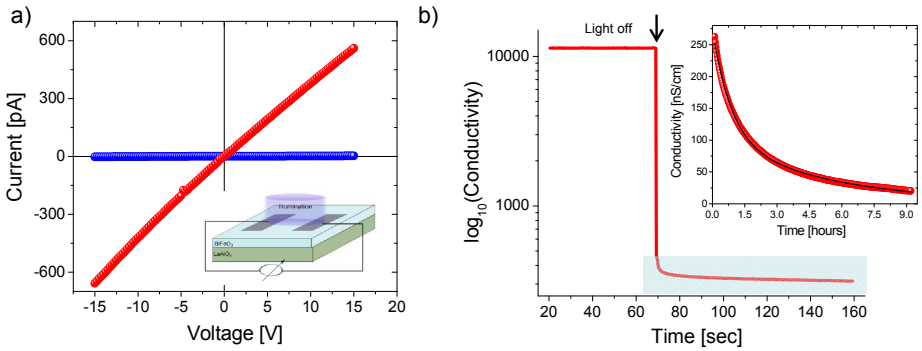

Figure 2: a) IV curves obtained before (blue) and after (red) illumination for a BFO film similar to the type shown in Fig. 1. The inset shows the measurement geometry. b) Logarithmic plot showing the sudden drop in conductivity when the light is switched off after illuminating for 20 mins (The plot shows only the initial few seconds of the drop). The inset shows an extended plot of the blue area which indicates a gradual decay of dark conductivity measured as a function of time; the black line represents the fit with Eq. 1

approximately 240 nS/cm. This is almost three orders of magnitude higher than the pristine conductivity value - a tremendous change in conductivity. In a separate measurement, this enhanced conductivity was measured as a function of time and is shown in Figure 2b. A gradual exponential-like decay of the conductivity was observed with time. Interestingly, the decay time is abnormally large and the high conductivity state persists for several thousands of seconds till it reaches the conductivity value of the pristine state. In the simplest of cases, it can be assumed that such a behavior follows a double exponential decay:[17,18]

$$\sigma(t) = \sigma_{01} exp\frac{-t}{\tau_1} + \sigma_{02} exp\frac{-t}{\tau_2} \tag{1}$$

where σ is the conductivity, t is time, and τ_1 and τ_2 are the two decay times for the charge carriers. The fit of equation 1 with the data in Figure 2b (inset of Figure 2b) yields two decay times $\tau_1$and τ_2 which are approximately 52 mins and 5.4 hours, respectively. We must emphasize here that these decay times cannot be considered to be a true characteristic of the material. In this approximation we are completely neglecting the existence of any sub-band level or any kind of thermally activated process. Nevertheless, the decay times are several orders of magnitude higher than the usual lifetimes of the carriers. Additionally, heating the sample to about 450 K and cooling down again to room temperature brings the conductivity back to the pristine state, or in other words resets the conductivity state to the pristine state. Such a drastic change in the conductivity at room temperature after switching off the illumination, and the possibility to revert back to the pristine state by heating the sample, clearly indicates to the presence of sub-band levels that can be activated by illumination and contribute to the conduction mechanism. As a result, the decay time of the conductivity is largely enhanced and is much higher than the usual lifetime of charge carriers.[17–19]

We assume that the origin of the persistent photoconductivity is a level or a distribution of levels that exist within the band gap of BFO, and are in proximity of the mobility edge. A possible mechanism can be charging of these levels with carriers by light, either directly

from the valence band or via conduction band and trapping. This will lead to a modification of the carrier statistics, especially the Fermi level. Consequently, some of the sub-band levels will change their character, from being ground states to trap levels or levels in thermal equilibrium with the allowed bands.

Spectral distribution

In order to validate such a mechanism, firstly we have to check for the existence of these levels. The required evidence may come from the spectral distribution of the photo-response. Figure 3 shows the spectral distribution of the normalized photoconductive response from a strained BFO film. The presence of a rather broad peak (marked by a star) between 550 and 650 nm, comprising of obviously two or more sub-peaks, is evident. This broad peak is a direct indication to the existence of optically and photoelectrically active levels in the band gap of the strained BFO film. Moreover, the photo-response increases continuously from about 505 nm till it peaks at approximately 420 nm. Firstly, this suggests that the band gap value is around 2.95 eV and, secondly, there is a distribution of sub-band levels resulting in a continuous response between 505 nm and 420 nm. Although the spectral distribution of

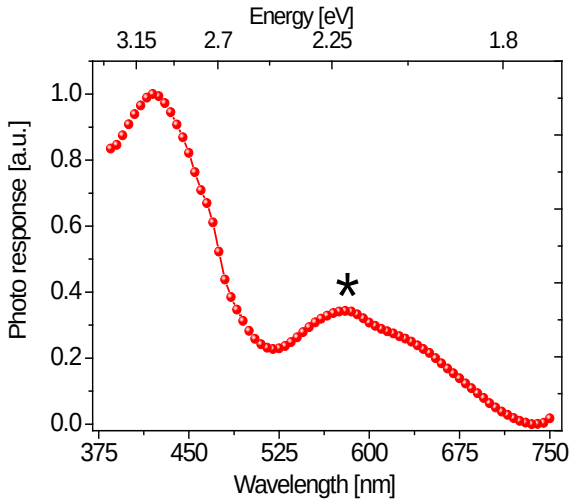

Figure 3: Normalized spectral distribution of the photo-response obtained from the same BFO film as in Fig. 1. The wavelength is scanned from 750 nm to 380 nm.

the photo-response indicates the existence of optically active sub-band levels which might be responsible for the PPC effect, we need to confirm further that these levels are also electronically active and hence can influence the conductivity of the material. We thus employed a technique to investigate thermally stimulated currents (TSC), to further elucidate on a sub-band level-mediated conduction in the strained BFO films.

Thermally stimulated currents

Measurement of thermally stimulated currents (TSC) is an efficient way of detecting and analyzing sub-band level mediated conduction mechanisms in dielectric and insulating materials.[20] The measurement involves stimulating the material at lower temperatures (in this case by light) followed by rapid cooling. Thereafter, the temperature is gradually increased with a simultaneous measurement of the current. The method has been employed intensively at the eve of semiconductor physics for characterizations of trap levels in typical semiconductors such as silicon and germanium as well as in wide band gap semiconductors such as CdS.[21,22] Figure 4a shows the TSC spectrum when the sample had been (red), and had not been illuminated (blue) for 20 minutes at room temperature. There is an evident difference between the two spectra, which is an effect of illuminating the sample at room temperature. The appearance of a peak in the TSC measurement clearly validates the role of sub-band levels in the conduction mechanism. The peak in the TSC measurement can be explained by the help of the schematic shown in Figure 4(c-e) where E_c and E_v indicate the conduction and valence band edges, respectively. At room temperature when the BFO film is illuminated by light with energy higher than the band gap, non-equilibrium free carriers generated from the valence band will be trapped at the sub-band levels (Figure 4c). The filling up of these levels will cause the quasi-Fermi level of electrons E_f^n to move further up above this trap level. When the material is rapidly cooled down, the carriers are frozen in their respective states and E_f^n moves further towards the allowed band edge (Figure 4d). Thereafter,

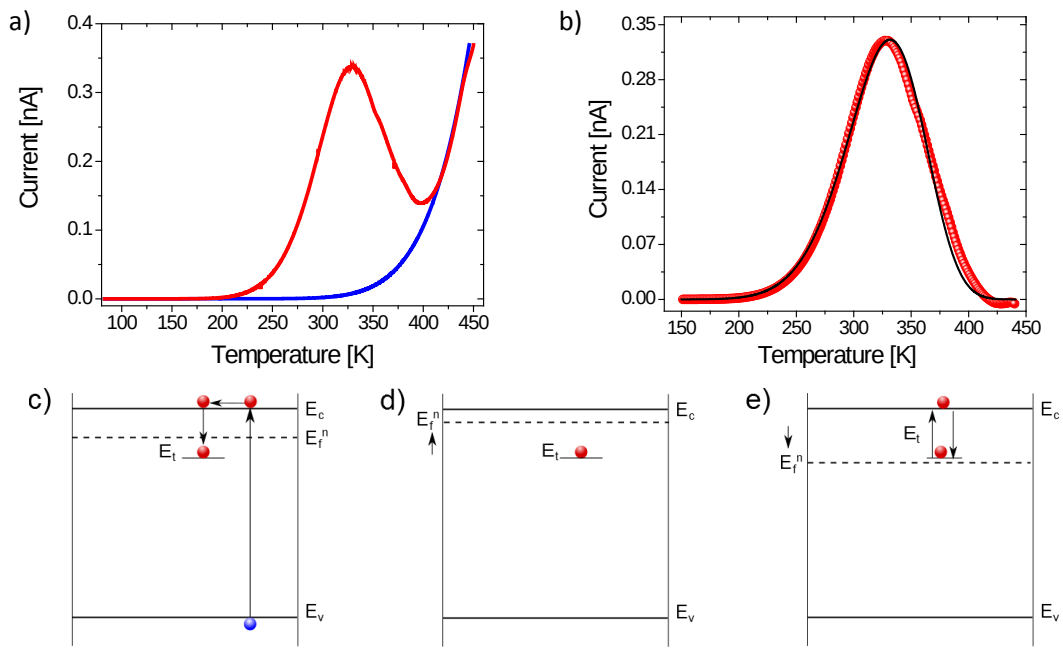

Figure 4: a) TSC measurement when the film had been (red), and had not been (blue) subjected to 20 min. of illumination at room temperature. b) Fitting of the TSC peak (red) with Equation 2 (black). Schematic showing band diagrams when c) the film is under illumination (h$\upsilon \geq E_c$) at room temperature with red and blue dots depicting electron and holes, respectively; d) the film is rapidly cooled, E_f^n rises above E_t and the carriers are trapped; and e) the film is heated at a constant rate due to which E_f^n moves towards the middle of the band gap and consequently the previously trapped carriers come into equilibrium with E_c.

as the material is gradually heated, E_f^n moves towards the middle of the gap, and during this process crosses the sub-band level. As this happens, the carriers previously trapped in the level come into thermal equilibrium with the allowed bands (Figure 4e). Consequently, there are additional carriers available which result in a higher conductivity and thus higher current. The current begins to increase at approx. 240 K (Figure 4a) and peaks at 330 K, beyond room temperature. From 240 K, the E_f^n level continues to sweep across the sub-band level with increasing temperature, till most of the carriers have been freed from the sub-band level and the recombination processes begin to dominate. Hence, the current after reaching a maximum value begins to decrease. The TSC measurement based on thermal emptying of carriers can be explained by an equation of the type:

$$J_{tsc} = J_{t0}\tau P_t exp\left[\frac{-1}{\gamma}\int P_t dt\right] \tag{2}$$

where J_{tsc} is the current due to the charge carriers freed from a trap level, J_{t0} is the current due to the trapped carriers at 0K, τ is the lifetime of a carrier, γ is the heating rate, and P_t is the probability of a carrier to escape from a trap level. The probability is temperature dependent and is given by:

$$P_t = N_c\beta_n exp\left[\frac{-E_a}{kT}\right] \tag{3}$$

where N_c is the number of free states available in the conduction band, β_n is the capture coefficient of the trap level and E_a is the activation energy of the trap level. By fitting the measured data with equation 2 as shown in Figure 4b, the activation energy E_a is found to be 0.26 eV. Keeping in perspective the spectral distribution of the photo-response, one might suspect that the level is situated at about 0.26 eV below E_c.

Discussions

Based on the measurements of the spectral distribution and the TSC, the conduction mechanism in strained BFO films can be explained. The spectral distribution clearly suggests the existence of sub-band levels in the band gap of BFO. One of the levels seems to be rather deep at an energy level of 2.2 eV below E_c and encountered while the wavelength is scanned between 550 to 650 nm. The peak due to this level is rather broad which could be due to the presence of a band of levels. The onset of photoconduction at an energy of approximately 2.45 eV, or 505 nm, indicates the presence of a level that is further in the vicinity of E_c. The absence of a distinct peak suggests that the level, or the band levels, within this energy range are in close proximity with the bottom of the conduction band. This is further validated by the TSC measurement where a level at an energy 0.26 eV below E_c was obtained. The persistent photoconductivity observed at room temperature is a direct consequence of pumping carriers into sub-band levels by light. The levels, which in the pristine state are empty, are pumped, which changes the carrier statistics by varying the Fermi level. So, while initially these levels are not contributing to the overall conduction mechanism, after illumination they come into thermal equilibrium with E_c and participate in the conduction. The trap levels filled by initial illumination will gradually empty and eventually reset the Fermi level to the initial level. It is worth noting that cathodoluminescence studies for the non-strained rhombohedral BFO have shown the presence of levels at 2.4 and 2.2 eV.[23] The effect of these levels on the macroscopic conducting properties of rhombohedral BFO has never been proven although their effect on generation and recombination of photo-generated charge carriers has been shown by microscopic studies.[24] Here we have shown that in the monoclinic phase, which is stabilized by strain, one level is placed in the range between 2.47 eV and E_c, and the other one at 2.2 eV. The presence of these levels in both phases of BFO proves the inherent nature of these levels in BFO. Nevertheless, in the strained BFO films, the effect of these levels on the conducting properties is massive. It can be speculated that due to the monoclinic phase, and hence a different arrangement of

atoms, the potential surrounding these levels is largely affected. This eventually affects their capture cross-section. The capture cross-section of a level determines its ability to capture and re-emit the carriers.[18] Consequently the effect of these levels on the conduction mechanism is more evident than in the rhombohedral phase. The present study indicates that the conductivity of strained BFO is dependent on the history of the sample, particularly if the sample has been or not illuminated with above-band gap light. This might also provide an explanation for the high conductivity in strained BFO films which has been seen as a primary concern for the ferroelectric characterization of these films.

Conclusions

In summary, an enhanced and persistent photoconductivity in strained BFO films is shown. Analyses of the spectral distribution revealed the presence of sub-band levels and their influence on the photo response. A peak in the TSC measurement explicitly proves the effect of a sub-band level on the macroscopic conduction mechanism. Henceforth, the charging of the trap levels by illumination and their subsequent thermal emptying is found to be at the origin of persistent photoconductivity in strained BFO films. Interestingly, since this effect is observed only in strained films of BFO, one might perceive a role of the strain in modulating the capture cross-section of the level that makes it more active in strained films than in relaxed films. Incidentally in the case of strained BFO films the position of the Fermi level with respect to the trap levels makes these levels to be active exactly at room temperature. The manifestation of such a phenomenon in a ferroelectric material opens the door to the possibility of tuning the conduction mechanism of materials by light and provides these materials with an added functionality.

Methods

Sample fabrication

Approximately 110 nm thick BFO films were deposited via pulsed laser deposition on $(001)_{pc}$-oriented LAO substrates. The films were deposited by ablating a BFO ceramic target with a laser energy of 0.35 J/cm^2. The films were deposited at a substrate temperature of 650 °C and a laser repetition rate of 10 Hz. Subsequently, the films were cooled down at 15 K/min under an O_2 partial pressure of 200 mbar. Thereafter, patterned electrodes of platinum were fabricated on top of the films by following conventional photolithography steps and sputtering. The distance between the electrodes was approximately 15 μm.

Photoelectrical measurements

The gap between the electrode was uniformly illuminated by a laser (Newport LQA405-85E) of wavelength 405 nm (hυ=3.06 eV) with a maximum power of 80 mW. The current was measured simultaneously using a high input impedance electrometer (Keithley 6517). For the spectral distribution, the wavelength was varied by using a monochromator in tandem with a white light lamp and simultaneous measurement of photocurrent under an applied bias voltage. The photocurrent at each wavelength was then normalized with the power available for every wavelength, to obtain the effective photoresponse. All the electrical and photoelectrical measurements were performed in an optical cryostat (Janis VPF-700).

Thermally stimulated current measurement

For these measurements, the sample was illuminated by a laser of wavelength $\lambda = 405$ nm, under a bias voltage of 10 V at room temperature. The resultant electric field is much lower than the coercive electric field for BFO grown on LAO.[7,25] The room temperature was chosen since it is also the temperature at which the persistent photoconductivity is observed. The sample was then cooled down rapidly under the bias voltage and was stabilized at 80 K. The

temperature of the sample was then increased at 5 K/min and the current was measured while maintaining the bias voltage.

Acknowledgement

The work was partly funded by DFG via SFB 762. A.B. is thankful to IMPRS (International Max Planck Research School, Halle, Germany) for the funding and support.

References

(1) Kubel, F.; Schmid, H. *Acta Crystallographica Section B Structural Science* **1990**, *46*, 698–702.

(2) Béa, H. et al. *Physical Review Letters* **2009**, *102*, 1–5.

(3) Zeches, R. J. et al. *Science* **2009**, *326*, 977–80.

(4) Ricinschi, D.; Yun, K.-Y.; Okuyama, M. *Journal of Physics: Condensed Matter* **2006**, *18*, L97–L105.

(5) Damodaran, A. R.; Liang, C.-W.; He, Q.; Peng, C.-Y.; Chang, L.; Chu, Y.-H.; Martin, L. W. *Advanced Materials* **2011**, *23*, 3170–5.

(6) Chen, Z.; Luo, Z.; Huang, C.; Qi, Y.; Yang, P.; You, L.; Hu, C.; Wu, T.; Wang, J.; Gao, C.; Sritharan, T.; Chen, L. *Advanced Functional Materials* **2011**, *21*, 133–138.

(7) Vasudevan, R. K.; Liu, Y.; Li, J.; Liang, W.-I.; Kumar, A.; Jesse, S.; Chen, Y.-C.; Chu, Y.-H.; Nagarajan, V.; Kalinin, S. V. *Nano Letters* **2011**, *11*, 3346–54.

(8) Jiang, A. Q.; Wang, C.; Jin, K. J.; Liu, X. B.; Scott, J. F.; Hwang, C. S.; Tang, T. A.; Lu, H. B.; Yang, G. Z. *Advanced Materials* **2011**, *23*, 1277–1281.

(9) Mulders, A. M. *Nature Physics* **2013**, *9*, 398399.

(10) Sando, D. et al. *Nature Materials* **2013**, *12*, 641–646.

(11) Yamada, H.; Garcia, V.; Fusil, S.; Boyn, S.; Marinova, M.; Gloter, A.; Xavier, S.; Grollier, J.; Jacquet, E.; Carretero, C.; Deranlot, C.; Bibes, M.; Barthelemy, A. *ACS Nano* **2013**, *7*, 5385–5390.

(12) Lu, H.-L.; Liao, Z.-M.; Zhang, L.; Yuan, W.-T.; Wang, Y.; Ma, X.-M.; Yu, D.-P. *Scientific Reports* **2013**, *3, doi: 10.1038/srep02870*.

(13) Tebano, A.; Fabbri, E.; Pergolesi, D.; Balestrino, G.; Traversa, E. *ACS Nano* **2012**, *6*, 1278–1283.

(14) Ohtomo, A.; Hwang, H. *Nature* **2004**, *427*, 423–426.

(15) Thiel, S.; Hammerl, G.; Schmehl, A.; Schneider, C. W.; Mannhart, J. *Science* **2006**, *313*, 1942–1945.

(16) Tarun, M. C.; Selim, F. A.; McCluskey, M. D. *Physical Review Letters* **2013**, *111*, 187403.

(17) Bube, R. H. *Photoelectronic properties of semiconductors*; Cambridge: Cambridge University Press, 1992.

(18) Bube, R. H. *Photoconductivity of Solids*; New York: John Wiley & Sons, INC., 1960.

(19) Rose, A. *Physical Review* **1955**, *97*, 322–333.

(20) Bräunlich, P., Ed. *Thermally stimulated Relaxation in Solids*; Springer-Verlag Berlin Heidelberg New York, 1979.

(21) Bube, R. H.; Thomsen, S. M. *The Journal of Chemical Physics* **1955**, *23*, 15–17.

(22) Bube, R. H.; Thomsen, S. M. *The Journal of Chemical Physics* **1955**, *23*, 18–25.

(23) Hauser, A. J.; Zhang, J.; Mier, L.; Ricciardo, R. A.; Woodward, P. M.; Gustafson, T. L.; Brillson, L. J.; Yang, F. Y. *Applied Physics Letters* **2008**, *92*, 222901.

(24) Alexe, M. *Nano Letters* **2012**, *12*, 2193–2198.

(25) You, L.; Chen, Z.; Zou, X.; Ding, H.; Chen, W.; Chen, L.; Yuan, G.; Wang, J. *ACS Nano* **2012**, *6*, 5388–94.

Graphical TOC Entry